Volume 13, Issue 1
February 2024

ITEE Journal
Information Technology & Electrical Engineering

ISSN: - 2306-708X

Scrutinization of Newton-GMRES Method For the Solution Of Thermal Elastohydrodynamic Lubrication Line Contact Problem With Grease A

[1]Vishwanath B. Awati, [2] Parashuram M. Obannavar, and [3]Mahesh Kumar N.

[1,2,3]Department of Mathematics, Rani Channamma University, Belagavi-591156, Karnataka, India

E-mail: [1]awati.vb@rcub.ac.in, [2]omparashu967@gmail.com,[3]maheshkumarnmk98@gmail.com

ABSTRACT

In the present work, we analyze the thermal Elastohydrodynamic lubrication (EHL) of line contact problem with grease as lubricant. The non-Newtonian Herschel-Bulkley model is employed to derive the governing equations of the physical problem. The governing mathematical model is analyzed numerically for smooth as well as rough surfaces. The various effects of temperature on pressure and film thickness profile are discussed in detail. The leading equations viz., Reynolds, film thickness, load balance and energy equations along with appropriate boundary constraints are discretized by using second order finite difference approximations. The resulting systems of non-linear algebraic equations were solved numerically through Newton-GMRES method with Daubechies D6 wavelet as pre-conditioner. The multilevel multi integration (MLMI) technique is employed to compute the film thickness. The obtained results are illustrated through figures and tables. The comparison of isothermal and thermal film thickness profiles for various load and speed are presented. It shows that, the isothermal minimum film thickness is greater than compared to the thermal minimum film thickness, and as the flow index *n* increases the respective film thickness also increases.

Keywords:*EHL, MLMI, Herschel-Bulkley, Newton-GMRES method, Daubechies D6 wavelet*

1. INTRODUCTION

In the tribology components, the load is applied over a small contact region which results into high pressure generated within the contact region; it leads to deformation of the contacting surfaces. This phenomenon of lubrication is widely known as Elastohydrodynamic lubrication (EHL). In most of the machine components viz., cams, rolling bearing, tappets and gears etc. The various lubricants used in order to reduce the friction, wear and tear of machine elements, to increase the life of machine components. Grease is used as lubricant in 80-90% of the machine components. The properties offered by grease make it as efficient lubricant under the operating conditions, due to its complex structure it behaves as a non-Newtonian fluid. Also, grease is different from other lubricant as it formed by lubricating oil and thickening agent dispersed in it. The simulation of EHL line contacts with grease as a lubricant enabled to overcome the failure of these components.

Experimentally Poon [1] was first to study the EHL problem lubricated with grease, and noticed that the film thickness of grease is higher than the base oil. The similar observations are made in the study of Wen and Ying [2], illustrated with sophisticated experimental tools. Using optical interferometry, Astrom et al. [3] and Kaneta et al. [4] analyzed EHL problems with fully flooded grease as lubricant. Specifically, at the inlet region, grease [5–8] influences an equal or even more significant for the determination of film thickness profiles. The film thickness increases with increase in viscosity of base oil was studied through experiment by Kageyama et al. [9]. Magnetic transducer was used to measure film thickness of grease in EHL line contact problem by Aihora and Dowson [10]. The Herschel-Bulkely model was used to examine the fully flooded EHL problem with grease by Kauziorich and Greenwood [11] through experimentally as well as theoretically. EHL line contact problem with similar model as in [11] was considered and obtained more accurate film shape by Jonkisz and Freda [12].

Boardenet et al. [13] discussed the point contact EHL problem and viewed the two fluid layers at the inlet region. The film thickness expression presented by Baart et al. [14] was a function of soap concentration and temperature. The more advanced film thickness formula was proposed by Ding and Qian [15] for EHL line contact problem. Herschel-Bulkly model was used to study the EHL line contact problem by Cheng [16]. This model was utilized to study the influence of temperature and grease rheology on the fluid film thickness by Yoo and Kim [17]. Karthikeyan et al. [18] shows the effect of temperature and speed on the nature of grease flow and film formation in EHL point contact. The review article of Lugt [19] revealed all the aspects of grease lubrication in rolling bearings. Awati and Naik [20] examined the EHL line contact problem with grease as lubricant using Multigrid method that comprises of Herschel-Bulkly model. The effect of electric double layer on EHL line contact problem is analyzed numerically by Awati et al. [21]. Zhang et al. [22] discussed the numerical solution of EHL finite line contact by considering the Ostwald model, predicting the film thickness by neural and genetic algorithms. Li et al. [23] analyzed the evolution of grease film with glass revolutions in rolling EHL contacts. The mixed lubrication of point contact problem was studied by Yang et al. [24] and the calculated film thickness for smooth and rough surfaces.

In general, contacting surfaces are no smooth in nature. Over the years many investigators studied the effect of surface roughness on EHL contacts. Three types of surface roughness found in the literature; viz., longitudinal, transverse and isotropic. Isotropic asperity presents randomly distributed and does not have apparent directions. The hydrodynamic fluid flow is governed by surface asperity these effects lubricant performance. Stochastic model and deterministic model are

Volume 13, Issue 1
February 2024

ITEE Journal
Information Technology & Electrical Engineering

ISSN: - 2306-708X

widely used in the analyses of hydrodynamic and elastohydrodynamic lubrication.

In stochastic model, it considers some statistical parameters to study the effect of surface asperity on contacting surfaces as well as properties of lubricant. To find the effect of surface roughness on hydrodynamic lubrication, researchers like Greenwood and Williamson [25], Greenwood and Tripp [26], Patir and Cheng [27] utilized the stochastic model. In order to explore the effect of surface asperities in EHL line contact problem deterministic model was used by Cheng [28]. The effect of temperature along with surface roughness in EHL problem was discussed by Sadeghi and Sui [29]. Further they applied Newton-Raphson method for calculating isothermal results and used control volume finite element method to solve energy equation to find the temperature. Numerical solution of point contact EHL problem was analyzed by Hu and Zhu [30]. They obtained 3-D surface asperity under various rolling/sliding parameters. Considering the average flow model of Patir Cheng [27] in mixed EHL problem was studied by Wang et al. [31], the computed results were agree with the findings of Hu and Zhu [30]. The experimental study of Lu et al. [33] considered both longitudinal and transverse surface asperity to analyze the thermal effects on elliptical EHL problem for different rolling/sliding conditions.

Akbarzadeh and Khonsari [34] discussed the effects of surface asperity on friction coefficients. EHL point contact problem along with surface asperity was studied by Sojoudi and Khonsari [35]. The effect of surface asperity on mixed lubrication of EHL line and point contact problems was discussed by Zhu and Wang [36] using deterministic model. The isothermal/thermal EHL point/ line contact problems with bio-based oil as lubricant on smooth and rough surface asperity were numerically discussed by Awati et al. [37], [38]. Awati and Kumar [39] considered the non-Newtonian piezo-viscous EHL line contact problem and determine the solution by using Newton-GMRES method with Daubechies D6 wavelet as pre-conditioner.

The study of thermal EHL problems gained much attention in the past few decades. The effect of temperature on EHL is demonstrated by Sternlicht et al. [40] and predicts the difference between isothermal and thermal film thickness. Cheng and Strenlicht [41] study the complete thermal EHL equations for Newtonian fluid. Greenwood and Kauzlarich [42] arrogate the shear heating and heat conduction into rollers to be the only mechanism of heat generation and removal inorder to simplify the energy equation. The similar energy equation is used by the Murch and Wilson [43] to discuss the thermal effects on film thickness. The importance of heating effect on the reduction of film thickness is explained by Ghosh and Hamrock [44]. The effect of temperature and non-Newtonian lubricant on the performance of EHL line contact problem was discussed by Salehizadeh and Saka [45].

The CFD model is used to explore the effect of thermal and shear thinning EHL line contact problem by Hartinger [46]. Wang and Yi [47] numerically discussed the transient thermal EHL analysis of an involute spur gear. By using Newton-Raphson and multigrid method, Khanittha and Jesda [48] determined the rough thermo-EHL with non-Newtonian lubricant. Jesda [49] numerically analyzed the effect of nano and micro particle additives on rough surface thermal EHL with non-Newtonian fluid. Zhang et al. [50] studied numerically the effect of finite line contact on bush-pin hinge pairs in industrial chains. The effect of temperature in micro-EHL finite line contact problem was analyzed by Liu et al. [51]. For highly loaded EHL contacts a new technique to predict traction was proposed by Liu et al. [52]. The experimental study on scale and contact geometry effects on friction in Thermal EHL problem was discussed by Philippon et al. [53]. Marian et al. [54] analyzed the point contact EHL problem by using the machine learning and artificial intelligence (AI) to predict the film thickness. Coupled finite element line contact solver was used to obtain the new coefficient formula for line contact EHL problem operating in the linear isothermal region was studied by Higashitani et al. [55].

1.1.KRYLOV SUBSPACE METHODS (KSM)

The discretization of partial differential equations (PDEs) by finite difference or finite element methods leads to a sparse linear system of equations. To solve these large sparse systems of equations there are many direct and iterative methods are available in the literature. Among them sparse direct solvers is one, which cannot be used for wide range of problems. The main focus of available iterative method is to minimize the number of iterations which is less than the order of coefficient matrix, in order to get the required solutions. Most of the large scale linear system of equations is solved by a preconditioned Krylov-subspace method, which is also an iterative method. Multigrid method is one of the most efficient finite difference methods but nowadays it is used as an inner iteration with a Krylov-subspace method as outer iteration.

Hestenes and Stiefel [56] introduced the Krylov subspace method as the direct method to solve large system of linear equations. But Ried [57], called these methods as an iterative method to solve the large-scale system of linear equations of the form $Ax = B$. Let x_0 be the initial approximation to the solution of system of equations and $r_0 = B - Ax_0$ be the initial residual error then

$$K_M(A, r_0) = span\left\{r_0, Ar_0, A^2 r_0, \ldots\ldots A^{M-1} r_0\right\} = K_M. \quad (1)$$

Where K_M be the Krylov-subspace of dimension M generated by A and r_0. The building blocks of Krylov-subspace methods are generated via Arnoldi, bi-Lanczos and complex symmetric Lanczos process. The Arnoldi process produces orthonormal basis vectors of Krylov-subspace, it never suffers from breakdown but computational costs increases with increase in the iteration number. Bi-Lanczos process obtains a orthogonal basis vectors of Krylov-subspace, the computational cost does not increases with number of iterations but breakdown occurs here and near the breakdown orthogonality property of basis vectors is lost. Hestenes and Stiefel [56] introduced the Conjugate gradient (CG) method and it is known as Krylov-subspace method. The review article of Golub and Leary [58] mentioned the history of CG method and it is derived from the Lanczos process. This method is applied when a matrix A is symmetric and positive definite. The Conjugate residual (CR)

Volume 13, Issue 1
February 2024

ITEE Journal
Information Technology & Electrical Engineering

ISSN: - 2306-708X

method proposed by Stiefel [59], it can be applied to symmetric indefinite matrix. The minimal residual (MINRES) method was introduced by Paige and Saunders [60], and CR method obtains the same approximate solutions. Lanczos process is used to achieve the minimization.

MINRES is generalized and named it as Generalized minimal residual (GMRES) method, the derivation of the method was given in [61]. The approximate solutions of linear system of equations would be $x_{\bar{n}}$ that minimizes $\|B - Ax_{\bar{n}}\|$ over the space $x_0 + \kappa_M(A, r_0)$. The Arnoldi process is used to generate orthonormal basis for the subspace $\kappa_M(A, r_0)$.

Let $V_{\bar{n}}$ be $\bar{n} \times \bar{n}$ matrix whose columns are basis for the subspace $\kappa_M(A, r_0)$ by Arnoldi process, since $x_{\bar{n}} \in x_0 + \kappa_M(A, r_0)$, we have

$$x_{\bar{n}} = x_0 + V_{\bar{n}} y_{\bar{n}},\ y_{\bar{n}} \in R^{\bar{n}}. \tag{2}$$

The residual vector for Eq. (2) can be expressed as

$$r_{\bar{n}} = r_0 - AV_{\bar{n}} y_{\bar{n}}. \tag{3}$$

Using the matrix representation of Arnoldi process $r_{\bar{n}}$ can be written as

$$r_{\bar{n}} = V_{\bar{n}+1}\left(\beta e_1 - H_{\bar{n}+1,\bar{n}} y_{\bar{n}}\right), \tag{4}$$

where, $\beta = \|r_0\|$, $H_{\bar{n}+1,\bar{n}}$ is Heisenberg matrix and ${V_{\bar{n}+1}}^H V_{\bar{n}+1} = I_{\bar{n}+1}$. is the identity matrix.

The 2-norm of residual vector is expressed as

$$\|r_{\bar{n}}\| = \left\|V_{\bar{n}+1}\left(\beta e_1 - H_{\bar{n}+1,\bar{n}} y_{\bar{n}}\right)\right\| = \left\|\beta e_1 - H_{\bar{n}+1,\bar{n}} y_{\bar{n}}\right\|. \tag{5}$$

By choosing a suitable $y_{\bar{n}}$ the 2-norm of the residual vector is minimized and $y_{\bar{n}}$ is written as

$$y_{\bar{n}} = \arg \min_{y \in R^{\bar{n}}} \left\|\beta e_1 - H_{\bar{n}+1,\bar{n}} y_{\bar{n}}\right\|. \tag{6}$$

The above mentioned $y_{\bar{n}}$ is computed by using Givens rotations. The GMRES is based on Arnoldi process of modified Gram-Schmidt type. As compared to other Krylov-subspace methods, GMRES is an attractive features viz., it never suffers from breakdown and residual 2-norm decreases monotonically and optimality regarding the residual 2-norm. The drawback of GMRES method is that, the number of iterations increases the computational costs and memory also increases linearly. To overcome this difficulty, restarted GMRES method is employed to obtain the solution. In this method, we fix the maximum number of iterations, once it is reached, and then use the restarted GMRES method, the previously obtained solution from GMRES will act as initial guess for the restarted GMRES method. The crucial point for successful application of GMRES revolves around the decision when to restart was given in [62], many researchers [63, 64, 65] discussed the same.

The complex structure and rheological characteristics of grease makes it for understanding EHL problems with grease as lubricant lags far behind. The numerical study of grease lubricant is quite less as compared to the experimental studies. Most of the numerical methods require large number of iterations to achieve converged solution. This is mainly due to large condition number of the matrix that occurs in solving large system of equations. The present study carries the numerical solution of EHL line contact problem with Herschel-Bulkley model. The numerical simulation consists of modified Reynolds, film thickness and load balance equations are solved simultaneously by using Newton-GMRES method with wavelet based pre-conditioner. In this method Newton's method is applied in the outer loop and GMRES with wavelet based pre-conditioner is used in the inner loop for the solution. The obtained results were presented for both smooth and rough surfaces with various operating conditions.

2. GOVERNING EQUATIONS

The Herschel-Bulkley model is used to predict shear stress with grease as lubricant in the lubricating film is expressed as

$$\tau = \pm\left[\tau_y + \eta_s \left|\dot{\gamma}\right|^n\right], \tag{7}$$

where τ_y is the yield stress, η_s is the viscosity of grease, $\dot{\gamma}$ is the shear rate and n is the flow index. The modified form of Reynolds equation is considered in an account of flow of grease between two cylinders (steady state, isothermal, incompressible and laminar). The pressure varies along the flow direction (x-direction).The modified Reynolds equation is given by (Yoo and Kim [17])

$$\left(\frac{1}{\eta}\frac{dp}{dx}\right)^m \left(1 - \frac{h_p}{h}\right)^{m+1} \left(1 + \frac{1}{m+1}\frac{h_p}{h}\right), \quad -\frac{K}{h^{m+2}}(h - h_0) = 0 \tag{8}$$

where $K = 2^{3m+1}(m+2)U\left(\frac{\pi}{8W}\right)^{m+1}$, η is the viscosity of grease, h is the film thickness, h_p is the width of the plug flow and $m = 1/n$.The dimensionless parameters used in the present study becomes

$$X = \frac{x}{b},\ H = \frac{hR}{b^2},\ P = \frac{p}{p_h},\ \tau_y = \frac{\tau_y}{\tau_{y0}},\ T_y = \frac{\tau_{y0}}{p_h},\ \bar{\eta} = \frac{\eta}{\eta_0},\ U = \frac{\eta_0^m u_s}{(E)^m R},\ W = \frac{w}{ER}. \tag{9}$$

The non-dimensional Reynolds equation can be written in the form

$$\left(\frac{1}{\bar{\eta}}\frac{dP}{dX}\right)^m \left(1 - \frac{H_p}{H}\right)^{m+1} \left(1 + \frac{1}{m+1}\frac{H_p}{H}\right), \quad -\frac{K}{H^{m+2}}(H - H_0) = 0 \tag{10}$$

Taking the last term to RHS and rearranging the terms, we get

$$\xi\left(\frac{dP}{dX}\right)^m = (H - H_0), \tag{11}$$

where, $\xi = \frac{H^{m+2}}{K}\left(\frac{1}{\bar{\eta}}\right)^m \left(1 - \frac{H_p}{H}\right)^{m+1} \left(1 + \frac{1}{m+1}\frac{H_p}{H}\right)$,

Volume 13, Issue 1
February 2024

ITEE Journal
Information Technology & Electrical Engineering

ISSN: - 2306-708X

$$H_p = \begin{cases} H & \text{if } \dfrac{dP}{dX} = 0 \\ 2T_y\sqrt{\dfrac{\pi}{8W}}\dfrac{\bar{\tau}_y}{dP/dX} & \text{Otherwise.} \end{cases} \quad (12)$$

Now, differentiating the Eq. (11) with respect to X, we get

$$\frac{d}{dX}\left(\xi\left(\frac{dP}{dX}\right)^m\right) = \frac{dH}{dX}. \quad (13)$$

Eq. (13) represents the modified Reynolds equation for grease as lubricant. The boundary constraints for the pressure are given in dimensionless form as

$P(X) = 0$, at the inlet region $X = X_{in}$, and at the outlet region

$$\frac{dP}{dX} = 0, \text{ at } X = X_{out}. \quad (14)$$

The fluid film thickness equation in dimensionless form can be written as

$$H(X) = H_0 + \frac{X^2}{2} - \frac{2}{\pi E}\int_{X_{in}}^{X_{out}} P(X')\ln(X - X')dX' + \Re, \quad (15)$$

where $\Re = \hat{A}\sin\left(\dfrac{2\pi X_i}{\hat{l}}\right)$, $\Re$ is the sinusoidal roughness, $\hat{A}$ is the amplitude, and $\hat{l}$ is the wavelength. The Roelands [66] viscosity-pressure-temperature relation is used in the present analysis and it can be written in dimensionless form as

$$\bar{\eta} = \exp\begin{Bmatrix}\left[\ln(\eta_0) + 9.67\right]\left\{-1 + (1 + 5.1\times10^{-9}\, p_h P)^{0.68}\right\} \\ -\gamma T_0(T^* - 1)\end{Bmatrix}. \quad (16)$$

The yield stress of grease, it can be written in non-dimensional form as

$$\bar{\tau}_y = \exp\begin{Bmatrix}\left[\ln(\tau_0) + 9.67\right]\left\{-1 + (1 + 5.1\times10^{-9}\, p_h P)^{0.68}\right\} \\ -\gamma T_0(T^* - 1)\end{Bmatrix} \quad (17)$$

where γ is the temperature-viscosity coefficient of lubricant, T_0 is the initial temperature and T^* is the dimensionless temperature. The density-pressure-temperature is expressed as

$$\rho^* = 1 + D_0 T_0\left(T^* - 1\right). \quad (18)$$

where, $D_0 = -0.00065$. The force balance equation in dimensionless form is expressed as

$$\int_{X_{in}}^{X_{out}} P(X)dX = \frac{\pi}{2}. \quad (19)$$

2.1. ENERGY EQUATION

The energy equation is used to calculate the temperature in the contact region which can be written in the form of

$$\rho c_p u\frac{\partial T}{\partial x} = k\frac{\partial^2 T}{\partial z^2} - \frac{T}{\rho}\frac{\partial \rho}{\partial T}u\frac{\partial p}{\partial x} + \eta\left(\frac{\partial u}{\partial z}\right)^2 \quad (20)$$

By using the dimensionless parameters the energy equation can be written in the form of

$$A\rho^* u^*\frac{\partial T^*}{\partial X} + B\frac{u^* T^*}{\rho^*}\frac{\partial \rho^*}{\partial T^*}\frac{\partial P}{\partial X} + C\frac{\partial^2 T^*}{\partial Z^2} + D\bar{\eta}\left(\frac{\partial u^*}{\partial Z}\right)^2 = 0. \quad (21)$$

where $A = \rho_0 c_p u_s T_0 / b$, $B = u_s p_h / b$, $C = -kT_0 R / b^2$, and $D = -\eta_0\left(\dfrac{u_s R}{b^2}\right)^2$. The relevant boundary conditions for Eq. (21) in dimensionless form can be expressed as

$$T^*_{usf} = 1 + \frac{k\sqrt{\eta_0 R}}{\sqrt{\pi\rho_1 c_1 u_1 E k_1 b^3}}\int_{-\infty}^{X}\frac{\partial T^*}{\partial Z}\frac{dS}{\sqrt{X - S}}, \quad (22)$$

$$T^*_{dsf} = 1 + \frac{k\sqrt{\eta_0 R}}{\sqrt{\pi\rho_2 c_2 u_2 E k_2 b^3}}\int_{-\infty}^{X}\frac{\partial T^*}{\partial Z}\frac{dS}{\sqrt{X - S}}. \quad (23)$$

3. DISCRETIZATION OF GOVERNING EQUATIONS

The computational domain for the present work is $X_{in} = -4$, $X_{out} = 1.5$ with $N=256$ uniform grid points are considered. The second order finite difference approximations are used to discretize the Reynolds, film thickness and load balance equations. The modified Reynolds equation Eq. (13) can be discretized as

$$\begin{matrix}\dfrac{(\xi_i + \xi_{i+1})(P_{i+1} - P_i)^m - (\xi_i + \xi_{i-1})(P_i - P_{i-1})^m}{\Delta X^{1+m}} \\ -\dfrac{H_i - H_{i-1}}{\Delta X} = 0\end{matrix}, \quad (24)$$

where, $\Delta X = \dfrac{X_{out} - X_{in}}{N+1}$. The boundary conditions in discretized form as

$$P(X_{in}) = 0, \text{and} \frac{P(X_{out}) - P(X_{out-1})}{\Delta X} = 0. \quad (25)$$

The film thickness equation can be discretized as

$$H_i = H_0 + \frac{X_i}{2} - \frac{1}{\pi}\sum_{j=1}^{N} K_{ij}P_j + \hat{A}\sin\left(\frac{2\pi X_i}{\hat{l}}\right) \quad (26)$$

where, the kernel K_{ij} is given by

$$K_{ij} = -\left(i - j + \frac{1}{2}\right)\Delta X\left[\ln\left(\left|i - j + \frac{1}{2}\right|\Delta X\right) - 1\right] + \left(i - j - \frac{1}{2}\right)\Delta X\left[\ln\left(\left|i - j - \frac{1}{2}\right|\Delta X\right) - 1\right]. \quad (27)$$

The discretization of load balance equation becomes

$$\Delta X\sum_{i=1}^{N}\frac{(P_i + P_{i+1})}{2} = \frac{\pi}{2}. \quad (28)$$

The non-dimensional energy equation can be written in discretized form as

Volume 13, Issue 1
February 2024

ITEE Journal
Information Technology & Electrical Engineering

ISSN: - 2306-708X

$$A\rho^* u^*\left(\frac{T^*_{i,kk}-T^*_{i-1,kk}}{\Delta X}\right)+B\frac{T^*}{\rho^*}\frac{\partial\rho^*}{\partial T^*}\left(u^*\frac{P_{i,j}-P_{i-1,j}}{\Delta X}\right)+ C\left(\frac{T^*_{i,kk+1}-2T^*_{i,kk}+T^*_{i,kk-1}}{\Delta Z^2}\right)+D\overline{\eta}\left(\frac{u^*_{i,kk+1}-u^*_{i,kk}}{\Delta Z}\right)^2=0 \quad (29)$$

where, kk indicates the node number in the film thickness direction.

4. SOLUTION PROCEDURE

The non-linear systems of algebraic equations arises from the discretization of Reynolds, film thickness load balance equations and these equations are solved numerically by using Newton-GMRES method. Energy equation is solved by using finite difference with Gauss-Seidel iteration method. These systems of nonlinear equations are first solved using Newton's method in the outer loop, then obtained a system of linear equations $Ax=B$, are solved using GMRES method in the inner loop. The matrix *A* is usually dense, sparse, and non-symmetric in nature and condition number is large, thus GMRES method slowly converges. In order to avoid this drawback, the preconditioned technique is utilized by Ford et al. [66]. In our computation a suitable pre-conditioner (Daubechies D6 wavelet) is implemented to the matrix *A* in order to reduce the condition number to get converged solution in few iterations.

5. RESULTS AND DISCUSSION

The isothermal and thermal steady state EHL line contact problem with grease as lubricant is analyzed by using Newton-GMRES method. The leading equations are discretized using second order finite difference method. The resultant systems of non-linear algebraic equations are solved simultaneously using Newton-GMRES method with Daubechies D6 wavelet as pre-conditioner. The effect of temperature, dimensionless speed (*U*), load (*W*) on film thickness and pressure is analyzed with different flow index. Also the effect of sinusoidal roughness on pressure and film thickness is studied in detail by considering uniform grids size $N=257$. The operating parameters are taken from Yoo and Kim [17].

Fig.1 illustrates the film thickness profiles for various flow index *n* at a constant speed $U=1.0181E-11$ and load $W=4.5249E-05$, it is observed that, minimum film thickness decreases with decrease in the value of flow index *n*. For *n=1* lubricant behaves as Newtonian fluid, the film thickness profiles of Newtonian fluid is higher than the grease oil. The pressure and film thickness profiles for various speed $U=5.9050E-12,\ 1.0181E-11,\ 1.6968E-11,\ 2.3756E-11.$ at a constant load $W=4.5249E-05$ and $n=1$ is depicted in Fig. 2. It is noticed that, speed increases, the pressure spike and minimum film thickness increases.

Fig. 3 shows the pressure profiles for different load $W=2.2624E-05,\ 4.5249E-05,\ 9.0498E-05,\ 1.3575E-04$ with a constant speed $U=1.0181E-11$ and $n=1$. It predicts that, pressure spike decreases with increase in the dimensionless load. Film thickness distributions are depicted in Fig. 4, for various values of dimensionless load $W=2.2624E-05,\ 4.5249E-05,\ 9.0498E-05,\ 1.3575E-04$ at a constant speed $U=1.0181E-11$ with $n=1$. It shows that, the minimum and central film thickness decreases with increase in load parameter.

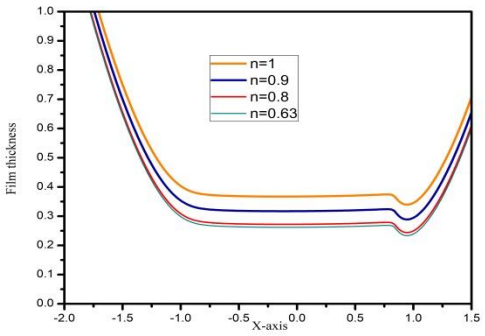

Fig. 1 Film thickness profiles for various flow index at a constant load $W=4.5249E-05$ and speed $U=1.0181E-11$.

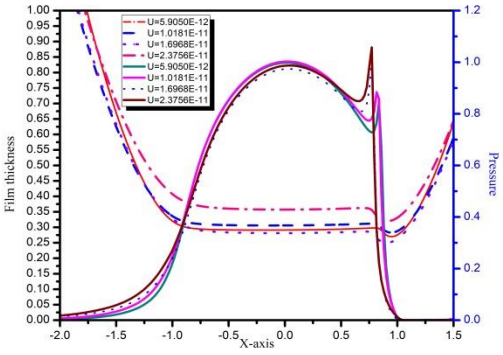

Fig. 2 Pressure and film thickness profiles for different speed with constant load $W=4.5249E-05$ and $n=1$.

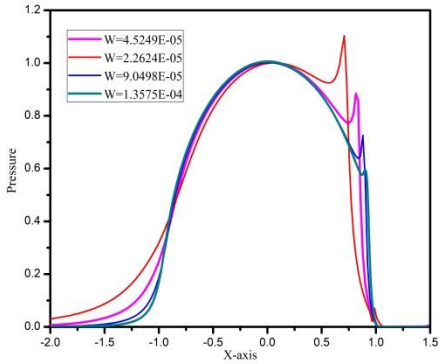

Fig. 3 Pressure distributions for various load at a constant speed $U=1.0181E-11$ and $n=1$.

Volume 13, Issue 1
February 2024

ITEE Journal
Information Technology & Electrical Engineering

ISSN: - 2306-708X

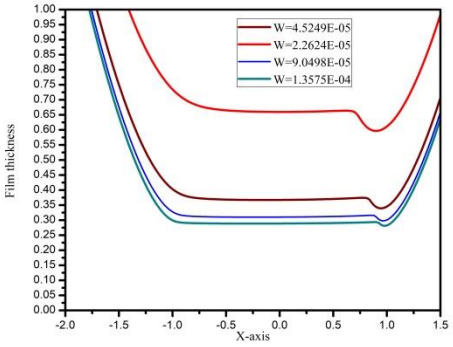

Fig. 4 Film thickness profiles for different load with a constant speed $U = 1.0181E-11$ and $n = 1$.

The non-Newtonian pressure and film thickness profiles are demonstrated in Figs. 5 and 6 respectively, for various speed at a constant load $W = 4.5249E-05$ and $n = 0.63$. These figures show the similar profiles as that of Newtonian fluid. Figs. 7 and 8 depicts, the non-Newtonian pressure and film thickness distributions respectively, for various load with a constant speed and n=0.63. It is observed that, pressure spike and film thickness decreases with increase in load in case of non-Newtonian fluid.

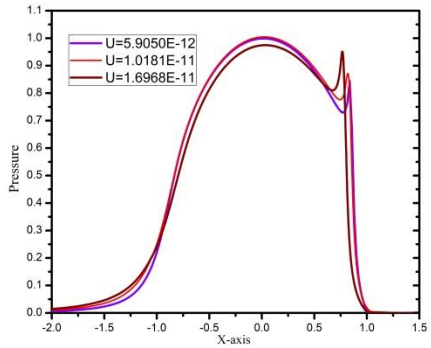

Fig. 5 Pressure profiles for various speed at a constant load $W = 4.5249E-05$ and $n = 0.63$.

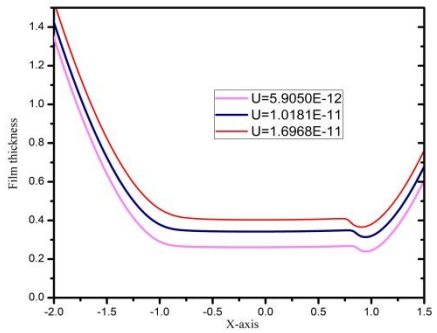

Fig. 6 Film thickness distributions for varying speed with a constant load $W = 4.5249E-05$ and $n = 0.63$.

The sinusoidal roughness is considered in the present study, the effect of roughness on pressure and film thickness is investigated in detail with amplitude $\hat{A} = 0.05$ and wavelength $\hat{l} = 0.05$. The pressure and film thickness profiles are demonstrated in Fig. 9 for high speed $U = 2.3756E-11$ and load $W = 4.5249E-05$ with $n = 1$. Pressure spike and the bulge in the film thickness are noticeable. For the non-Newtonian pressure and film thickness shows similar characteristics, as those are depicted in Fig.10 for high speed $U = 2.3756E-11$ and moderate load $W = 4.5249E-05$ with $n = 0.63$.

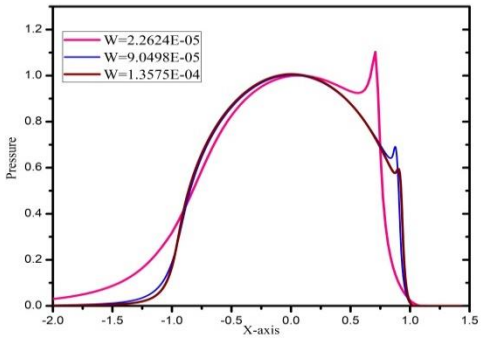

Fig. 7 Pressure distributions for varying load with a constant speed $U = 1.0181E-11$ and $n = 0.63$.

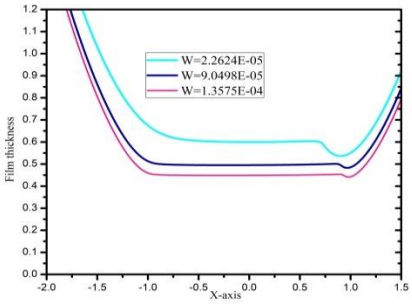

Fig. 8 Film thickness profiles for the different load at a constant speed $U = 1.0181E-11$ and $n = 0.63$.

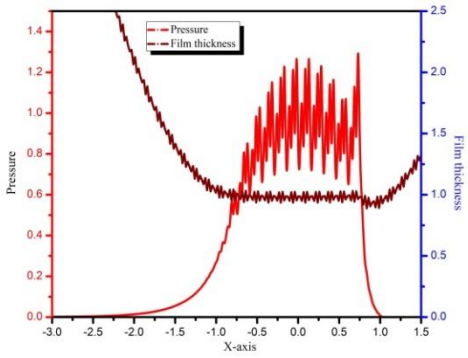

Fig. 9 Pressure and film thickness profiles for sinusoidal roughness at a speed $U = 2.3756E-11$, load $W = 4.5249E-05$ with $n = 1$.

Volume 13, Issue 1
February 2024

ITEE Journal
Information Technology & Electrical Engineering

ISSN: - 2306-708X

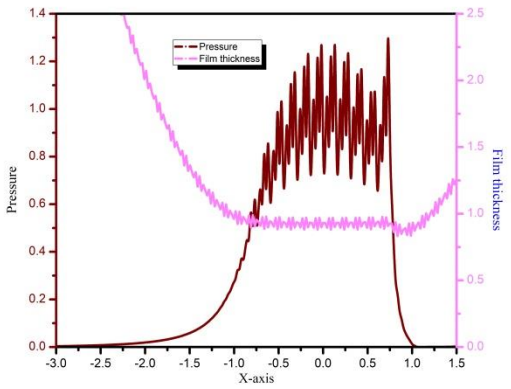

Fig. 10 Pressure and film thickness for sinusoidal roughness with speed $U = 2.3756E-11$, load $W = 4.5249E-05$ and $n = 0.63$.

Figs. 11 and 12 show the pressure and film thickness distributions for Newtonian and Non-Newtonian fluids respectively, at low load $W = 2.2624E-05$ and speed $U = 1.0181E-11$. Figs 13 and 14 shows the temperature profiles for the low speed ($U = 5.9050E-12$) and low load ($W = 2.2624E-05$) respectively for the flow index $n = 0.6$, and $n = 0.8$. these distributions predict that, the temperature in the contact region (middle layer) is higher than the surface temperatures.

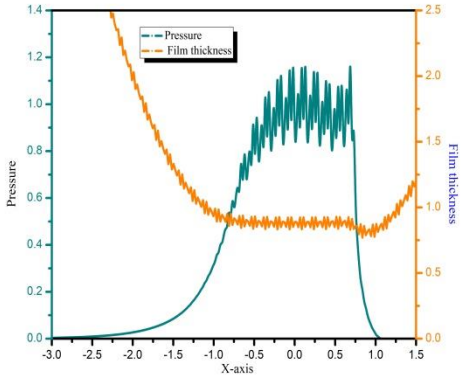

Fig. 11 Sinusoidal roughness Pressure and film thickness profiles for a low load $W = 2.2624E-05$ and moderate speed $U = 1.0181E-11$ with $n = 1$.

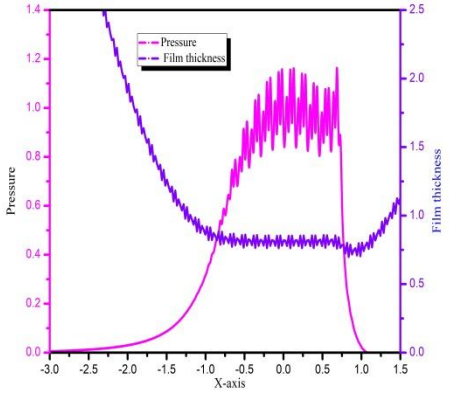

Fig. 12 Pressure and film thickness distributions for load $W = 2.2624E-05$, speed $U = 1.0181E-11$ with $n = 0.63$.

Pressure and film thickness distributions are depicted in Fig. 15 for the speed $U = 1.0181E-11$, load $W = 4.5249E-05$ with $n = 0.8$. It is observed that, thermal film thickness is smaller as compared to isothermal film thickness. In Fig. 16 the temperature profiles for the speed $U = 2.3756E-11$ and load $W = 4.5249E-05$ with different flow index $n = 0.6$ and 0.8 are illustrated. It is noticed that, the temperature peak increases with increase in the flow index.

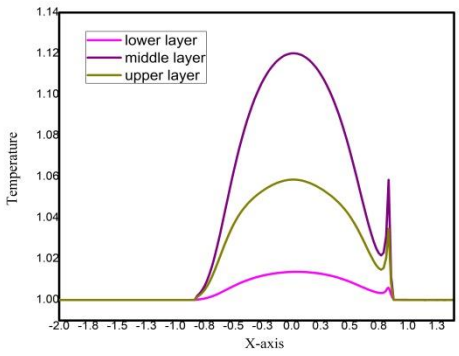

Fig. 13 Temperature distributions for the speed $U = 5.9050E-12$ at a constant load $W = 4.5249E-05$ with flow index $n = 0.6$.

Volume 13, Issue 1
February 2024

ITEE Journal
Information Technology & Electrical Engineering

ISSN: - 2306-708X

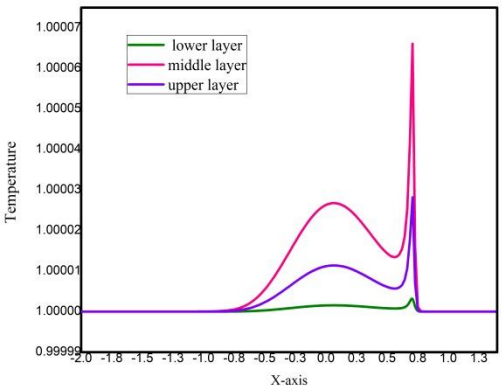

Fig. 14 Temperature profiles for the low load $W = 2.2624E-05$ at a constant speed $U = 1.0181E-11$ with flow index $n = 0.8$.

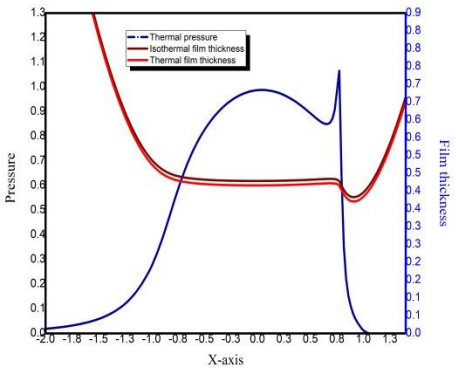

Fig. 15 Pressure and film thickness profiles for the isothermal and thermal cases at a constant speed $U = 1.0181E-11$ and load $W = 4.5249E-05$ with flow index $n = 0.8$.

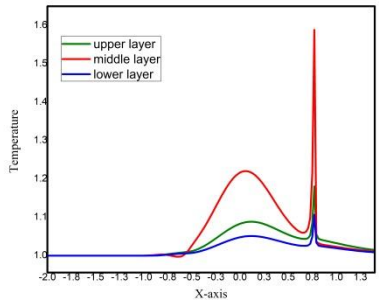

a) n=0.8

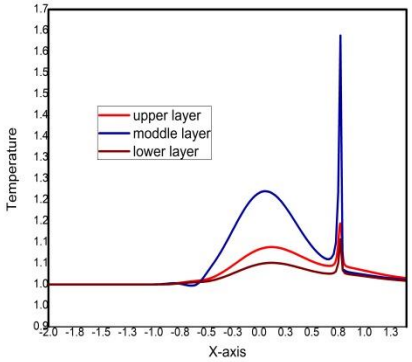

b) n=0.6

Fig. 16 a and b Temperature distributions for the high speed $U = 2.3756E-11$ at a constant load $W = 4.5249E-05$ with flow index $n = 0.8,0.6$ respectively.

Table 1presents the minimum (H_{min}) and central (H_{cen}) film thickness values for different speed and flow index. It is observed that, minimum and central film thickness decreases as the value of n decreases, and increases with increase in speed. Table 2 presents, the minimum and central film thickness values for different dimensionless load and flow index (n) at a constant speed. The minimum and central film thickness decreases with decrease in the flow index (n) and minimumand central film thickness decreases with increase in load. Table 3 shows the isothermal and thermal film thickness values fordifferent speed, it shows that isothermal minimum film thickness is larger than the thermal minimum film thickness and central film thickness is always larger than the minimum film thickness.

Table 1. Minimum film thickness values for different speed and flow index at a constant load

Dimension less load W	Dimension less speed U	Flow index					
		n=1 H_{min}	*n=0.8* H_{min}	*n=0.63* H_{min}	*n=1* H_{cen}	*n=0.8* H_{cen}	*n=0.63* H_{cen}
$4.5249E-05$	5.9050E-12	0.82 60	0.80 94	0.792 7	0.88 56	0.88 09	0.866 6
	1.0181E-11	0.83 05	0.81 15	0.801 5	0.91 54	0.89 84	0.888 5
	1.6968E-11	0.85 17	0.83 30	0.812 0	0.94 52	0.92 68	0.905 9
	2.3756E-11	0.88 88	0.85 85	0.832 7	0.98 81	0.95 89	0.933 3

Table 2 Minimum film thickness values for different load and flow index at a constant speed.

Dimensionless load W	Dimensionless speed U	Flow index					
		$n=1$ H_{min}	$n=0.8$ H_{min}	$n=0.63$ H_{min}	$n=1$ H_{cen}	$n=0.8$ H_{cen}	$n=0.63$ H_{cen}
2.2624E-05	$1.0181E-11$	0.7702	0.7296	0.6991	0.8895	0.8492	0.8189
9.0498E-05		0.7317	0.6967	0.6667	0.7996	0.7631	0.7346
1.3575E-04		0.7080	0.6730	0.6480	0.7708	0.7358	0.7108

Table 3. Comparison of isothermal and thermal minimum and central film thickness for various speed

Dimensionless load W	Dimensionless speed U	Flow index	Isothermal film thickness		Thermal film thickness	
			$\mathbf{H_{min}}$	$\mathbf{H_{cen}}$	$\mathbf{H_{min}}$	$\mathbf{H_{cen}}$
$4.5249E-05$	5.9050 E-12	$n = 0.6$	0.2481	0.2702	0.2372	0.2592
	1.0181 E-11		0.2833	0.3121	0.2650	0.2937
	2.3756 E-11		0.3831	0.4283	0.3707	0.4160

6. CONCLUSIONS

The following conclusions are drawn from the numerical solution of thermal EHL line contact problem with sinusoidal roughness by using grease as lubricant,

1. Newton-GMRES method with Daubechies D6 wavelet as pre-conditioner reduces the computational cost and convergence of the required solution with few numbers of iterations.
2. As the flow index n increases the fluid film thickness also increases.
3. Isothermal minimum film thickness is higher than that of thermal minimum film thickness.
4. As the speed increases the pressure spike move towards the Hertizian pressure region.
5. At the contact region the temperature is higher than that of the surface temperatures.

REFERENCES

[1] S-Y. Poon, "An experimental study of grease in elastohydrodynamic lubrication," 1972.

[2] S. Z. Wen, T. N. Ying, "A theoretical and experimental study of EHL lubricated with grease," 1988.

[3] H. Åstrom, O. Isaksson, E. Hoglund, "Video recordings of an EHD point contact lubricated with grease," 24, 179–84, 1991.

[4] M. Kaneta, T. Ogata, Y. Takubo, M. Naka, "Effects of a thickener structure on grease elastohydrodynamic lubrication films," J: Journal of Engineering Tribology, 214, 327–36, 2000.

[5] P. M. Cann, H. A. Spikes, "Film thickness measurements of lubricating greases under normally starved conditions," NLGI Spokesman, 52, 21–27, 1992.

[6] H. Åström, F. O. Östensen, E. Höglund, "Lubricating grease replenishment in an elasto-hydrodynamic point contact," Journal of Tribology, 115, 501–506, 1993.

[7] P. M. Cann, H. A. Spikes, "Visualization of starved grease and fluid lubricant films," Tribology Series, 30, 161–166, 1995.

[8] P. M. Cann, "Starved Grease Lubrication of Rolling Contacts," Tribology Transactions, 42(4), 867–873, 1999.

[9] H. Kageyama, W. Machidori, T. Moriuchi, "Grease lubrication in elastohydrodynamic contacts," NLGI Spokesman, 12, 72–81, 1984.

[10] S. Aihora, D. Dowson, "A study of film thickness in Grease lubricated elastohydrodynamic contacts," In: Proceedings of 5th Leeds-Lyon symposium on Tribology. Mechanical Engineering Publication, London, 1978, 104–115.

[11] J. J. Kauzlarich, J. A. Greenwood, "Elasto-hydrodynamic lubrication with Herskhel-Bulkley model grease," ASLE Transactions, 15, 269–277, 1972.

[12] W. Jonkisz, H. Krzeminiski-Freda, "The properties of elastohydrodynamic grease films," Wear, 77, 277–285, 1979.

[13] L. Boardenet, G. Dalmaz, J. P. Chaomleffel, F. Vergne, "A study of grease film thickness in elastohydrodynamic rolling point contacts," Lubrication Sciences, 2, 273–284, 1990.

[14] P. Baart, P. M. Lugt, B. Prakash, "Non-Newtonian effects on film formation in grease lubricated radial lip seats," Tribology Transactions, 53, 308–318, 2010.

[15] D. Dong, X. Qian, "A theory of elastohydrodynamic grease lubricated line contact based on a refined rheological model," Tribology International, 21, 261–267, 1988.

[16] J. Cheng, "Elastohydrodynamic grease lubrication theory and numerical solution in line contacts," Tribology Transaction, 37, 711–718, 1994.

[17] J. G. Yoo, K. W. Kim, "Numerical analysis of grease thermal elastohydrodynamic lubrication problems using the Herschel-Bulkley model," Tribology International, 30, 401–408, 1997.

[18] B. K. Karthikeyan, M. Teodorescu, H. Rahnejat,S. J. Rothberg, "Thermo-elastohydrodynamics of grease lubricated concentrated point contacts," Proc. Inst. Mech. E Part C J Mech. Eng. Sci., 224, 683–695, 2010.

[19] P. M. Lugt, "A review on grease lubrication in rolling bearings," Tribology Transactions, 52, 470–480, 2009.

[20] V. B. Awati, S. Naik, "A multigrid method for EHL line contact problem with Grease as lubricant," Mathematical Models in Engineering, 3, 126-134, 2017.

[21] V. B. Awati, P. M. Obannavar, N. Mahesh Kumar, "Newton-GMRES-Method for the Scritinization of electric double layer and surface roughness on EHL line contact problem," Journal of Mechanical Engineering and Sciences, 17, 9370-9382, 2023.

[22] K. Zhang, X. Peng, Y. Zhang, H. Zhou, "Numerical thermal analysis of grease-lubrication in limited line contacts considering asperity contact," Tribology International, 2019, doi: https://doi.org/10.1016/j.triboint.2019.01.026.

[23] L. I. Xinming, G. Feng, P. Gerhard, F. Yang,P. Yang, "Grease film evolution in rolling elastohydrodynamic lubrication contacts," Friction, 9, 179–190, 2021. ISSN 2223-7690, https://doi.org/10.1007/s40544-020-0381-4.

[24] J. Yang, D. Wang, W. Pengchong, P. Wei, "A mixed EHL model of grease lubrication considering surface roughness and the study of friction behavior," Tribology International, 154, 106710, 2021. https://doi.org/10.1016/j.triboint.2020.106710.

[25] J. Greenwood,J. Williamson, "Contact of Nominally Flat Surfaces," Proceedings of the Royal Society of London (A), 295, 1966, 300-319.

[26] J. Greenwood, J. Tripp, "The contact of two nominally flat rough surfaces," Proceedings of the institution of mechanical engineers, 185, 1970, 625-633.

[27] N. Patir, H. Cheng,"An Average Flow Model for Determining Effects of Three Dimensional Roughness on Partial Hydrodynamic Lubrication," ASME. J. of Lubrication Technology, 100, 12–17, 1978. https://doi.org/10.1115/1.3453103. 29

[28] F. Sadeghi, P. Sui, "Thermal Elastohydrodynamic Lubrication of Rough Surfaces," ASME. Journal of Tribology, 112, 341–346, 1990. https://doi.org/10.1115/1.2920262.

[29] L. Chang,"A deterministic model for line-contact partial elastohydrodynamic lubrication," Tribology International, 28, 75-84, 1995.

[30] Y. Hu, D. Zhu, "A Full Numerical Solution to the Mixed Lubrication in Point Contacts," ASME. Journal of Tribology, 122, 1–9, 2000. https://doi.org/10.1115/1.555322.

[31] Q. Wang, D. Zhu, H. Cheng, T. Yu, X. Jiang, S. Liu, "Mixed Lubrication Analyses by a Macro-Micro Approach and a Full-Scale Mixed EHL Model," ASME. Journal of Tribology, 126, 81–91, 2004. https://doi.org/10.1115/1.1631017.

[32] X. Lu, M. Khonsari, E. Gelinck, "The Stribeck Curve: Experimental Results and Theoretical Prediction," ASME. Journal of Tribology, 128, 789–794, 2006. https://doi.org/10.1115/1.2345406.

[33] P. Yang, J. Cui, Z. Jin, D. Dowson, "Influence of Two-Sided Surface Waviness on the EHL Behavior of Rolling/Sliding Point Contacts Under Thermal and Non-Newtonian Conditions," ASME. Journal of Tribology, 130, 041502, 2008. https://doi.org/10.1115/1.2958078.

[34] S. Akbarzadeh, M. Khonsari, "Performance of Spur Gears Considering Surface Roughness and Shear Thinning Lubricant," ASME. Journal of Tribology, 130, 021503, 2008. https://doi.org/10.1115/1.2805431.

[35] H. Sojoudi, M. Khonsari, "On the Behavior of Friction in Lubricated Point Contact with Provision for Surface Roughness," ASME. Journal of Tribology, 132, 012102, 2010. https://doi.org/10.1115/1.4000306.

[36] D. Zhu, J. Wang, "Effect of Roughness Orientation on the Elastohydrodynamic Lubrication Film Thickness," ASME. Journal of Tribology, 135, 031501, 2013. https://doi.org/10.1115/1.4023250.

[37] V. B. Awati, S. Naik,N. Mahesh Kumar, "Multigrid method for the solution of EHL point contact with bio-based oil as lubricants for smooth and rough asperity," Industrial Lubrication and Tribology, 70, 599–611, 2018.

[38] V. B. Awati, N. Mahesh Kumar,N. M. Bujurke, "Numerical solution of thermal EHL line contact with bio-based oil as lubricant," Australian Journal of Mechanical Engineering, 20, 231-244, 2022.

[39] V. B. Awati, N. Mahesh Kumar, "Newton-GMRES Method for the Solution of Piezo-Viscous Line Contact EHL Problem with Daubechies Wavelet as a Preconditioner," J. Mod. Ind. Manuf., 1, 4, 2022. DOI: 10.53964/jmim.2022004.

[40] B. Sternlicht, P. Lewis,P. Flyn, "Theory of Lubrication and Failure of Rolling Contacts," ASME /. Basic Eng., 83, 213-226, 1961.

[41] H. Cheng, B. Sternlicht, "A Numerical Solution for Pressure, Temperature, and Film Thickness Between Two Infinitely Long, Lubricated Rolling and Sliding Cylinders, Under Heavy Loads," ASME Journal of Basic Engineering, 695-707, 1965.

[42] J. Greenwood, J. Kauzlarich, "Inlet Shear Heating in Elastohydrodynamic Lubrication," ASME Journal of Lubrication Technology, 95, 417- 42, 1973.

[43] L. Murch, W. Wilson, "A Thermal Elastohydrodynamic Inlet Zone Analysis," ASME. Lubrication Technology, 97, 212-216, 1975.

[44] M. K. Ghosh, B. J. Hamrock, "Thermal Elastohydrodynamic Lubrication of Line Contacts," ASLE Transactions, 28, 159-171, 1984.

[45] H. Salehizadeh, N. Saka, "Thermal Non-Newtonian Elastohydrodynamic lubrication of rolling line contacts," Journal of Tribology, 113, 481-491, 1991.

[46] M. Hartinger, M. Dumont,S. Loannides,D. Gosman,H. Spikes, "CFD modeling of Thermal and Shear thinning elastohydrodynamic line contact," Journal of Tribology, 130, 0415031-16, 2008.

[47] Y. Wang, X. Yi, "Non-Newtonian transient thermo-elastohydrodynamic lubrication analysis of an involute spur gear," Lubrication Science, 22, 465-478, 2010.

[48] W. Khanittha, P. Jesda, "Effect of solid particle on rough Thermo-Elastohydrodynamic lubrication with Non-Newtonian Lubricant," Advanced Materials Research, 1044-1045, 305-309, 2014.

[49] P. Jesda, "Effect of Nano and Micro particle additives on Rough surface TEHL with Non-Newtonian Lubricant," 736, 45-52, 2015.

[50] M. Zhang, F. Wang, and Yang P. "A thermal EHL investigation for size effect of finite line contact on bush-pin hinge pairs in industrial chains," Industrial lubrication and Tribology, 72/5, 695-701, 2019.

[51] X. Liu, Z. Xin, J. Zhou, P. Yang, "Analysis of thermal dynamic micro-EHL considering bearing assembly temperature," Proc. IMech E Part J: Journal of Engineering Tribology, 235, 1283-1297, 2021.

[52] H. C. Liu, B. B. Zhang, N. Bader, C. H. Venner, G. Poll, "Simplified traction prediction for highly loaded rolling/sliding EHL contacts,"Tribology International, 148, 106335, 2020. https://doi.org/10.1016/j.triboint.2020.106335.

[53] D. Philippon, L. Martinie, P. Vergne, "Discussion on scale and contact geometry effects on friction in thermal EHL: twin disc versus ball-on-disc," Tribology international, 157, 106877, 2021.

[54] M. Marian, J. Mursak, M. Bartz, F. Profito, A. Rosenkranz, S. Wartzack, "Predicting EHL film thickness parameters by machine learning approaches," Friction, 11(6), 992-1013, 2023.

[55] Y. Higashitani, S. Kawabata, M. Björling, A. Almqvist, "A traction coefficient formula for EHL line contacts operating in the linear isothermal region," Tribology International, 180, 108216, 2023. https://doi.org/10.1016/j.triboint.2023.108216.

[56] M. R. Hestenes, E. Stiefel, "Methods of conjugate gradients for solving linear systems," J Res. Natl. Bureau Stand, 49, 409–436, 1952.

[57] J. Reid, "On the method of conjugate gradients for the solution of large sparse systems of linear equations," In: Reid JK(ed) Large sparse sets of linear equations. Academic Press, Cambridge, 1971, 231–254.

[58] G. Golub, D. O'Leary, "Some history of the conjugate gradient and Lanczos algorithms: 1948–1976," SIAM Rev., 31, 50–102, 1989.

[59] E. Stiefel, "Relaxations method enbester strategie zur lösung linearer gleichungssysteme," Comment. Mat.

[60] C. Paige, M. Saunders, "Solution of sparse indefinite systems of linear equations," SIAM journal on numerical analysis, 12, 617-629, 1975.

[61] Y. Saad, M. Schultz, "GMRES: A generalized minimal residual algorithm for solving non-symmetric linear systems," SIAM J. Sci. Stat. Comput., 7, 856–869, 1986.

[62] W. Joubert, "On the convergence behavior of the restarted GMRES algorithm for solving non-symmetric linear systems," Numer. Linear Algebra Appl., 1, 427–447, 1994.

[63] A. Baker, E. Jessup,T. Kolev, "A simple strategy for varying the restart parameter in GMRES(m)," J. Comput. Appl. Math., 230, 751–761, 2009.

[64] K. Moriya, T. Nodera, "The DEFLATED-GMRES(m, k) method with switching the restart frequency dynamically," Numer. Linear Algebra Appl., 7, 569–584, 2000.

[65] M. Sosonkina, L. Watson, R. Kapania, H. Walker, "A new adaptive GMRES algorithm for achieving high accuracy," Numer. Linear Algebra Appl., 5, 275–297, 1998.

[66] C. J. A. Roelands, J. C. Vlugter, H. I. Waterman, "The viscosity-temperature-pressure relationship of lubricating oils and its correlation with chemical constitution." 1963.

[67] J. Ford, K. Chen, L. Scales, "A new wavelet transform pre-conditioner for iterative solution of elastohydrodynamic lubrication problems," International Journal of Computer Mathematics, 75, 497-513, 2000. DOI: 10.1080/00207160008805000. 2000.

AUTHOR PROFILES

Dr. Vishwanath B. Awati received the degree in Mathematics from Karnataka University, Dharawad in 1994. He received his Ph. D. degree from Karnataka University, Dharawad. His research interest includes the MHD boundary layer flows of stretching/shrinking sheet problems, Elastohydrodynamic lubrication. Currently, he is Professor in the department of Mathematics at Rani Channamma University, Belagavi-591156, Karnataka, India.

Mr. Parashuram M. Obannavar received the degree in Mathematics from Rani Channamma University, Belagavi in 2018. He is pursuing Ph. D. under the guidance of Dr. Vishwanath B. Awati at Rani Channamma University, Belagavi. His research interest includes fluid dynamics, Elastohydrodynamic lubrication.

Dr. Mahesh Kumar N received the degree in Mathematics from University of Mysore, Mysore in 2004. He received his Ph. D. degree from Rani Channamma University, Belagavi. His research interest includes Fluid dynamics, Elastohydrodynamic lubrication. Currently, he is Assistant Professor in the department of Mathematics at Rani Channamma University, Belagavi-591156, Karnataka, India.